Published in J. Electron. Mater. 32, 855 (2003).

GROWTH OF GaN ON POROUS SiC AND GaN SUBSTRATES

C. K. Inoki and T. S. Kuan
Department of Physics, University at Albany, SUNY, Albany, NY 12222
C. D. Lee, Ashutosh Sagar, and R. M. Feenstra
Department of Physics, Carnegie Mellon University, Pittsburgh, PA 15213
D. D. Koleske
Chemical Processing Science Dept., Sandia National Laboratories, Albuquerque, NM 87185
D. J. Díaz, P. W. Bohn, and I. Adesida
Beckman Institute, University of Illinois, Urbana, IL 61801

ABSTRACT

We have studied the growth of GaN on porous SiC and GaN substrates, employing both plasma-assisted molecular beam epitaxy (PAMBE) and metalorganic chemical vapor deposition (MOCVD). For growth on porous SiC, transmission electron microscopy (TEM) observations indicate that the epitaxial GaN growth initiates primarily from surface areas between pores, and the exposed surface pores tend to extend into GaN as open tubes and trap Ga droplets. The dislocation density in the GaN layers is similar to, or slightly less than, that observed in layers grown on non-porous substrates. For the case of GaN growth on porous GaN the overgrown layer replicates the underlying dislocation structure (although considerable dislocation reduction can occur as this overgrowth proceeds, independent of the presence of the porous layer). The GaN layers grown on a porous SiC substrate were found to be mechanically more relaxed than those grown on non-porous substrates; electron diffraction patterns indicate that the former are free of misfit strain or are even in tension after cooling to room temperature. Significant changes in the stress of the overgrown layers on porous GaN were also found, as seen in line shifts of low-temperature photoluminescence spectra.

I. INTRODUCTION

Porous SiC and GaN have recently been explored as promising substrates to grow epitaxial SiC or GaN with reduced dislocation density [1-6]. Such porous materials are produced by anodizing n-type SiC in hydrofluoric acid under ultra-violet illumination [7]. Elongated pores with diameters 10 to 30 nm are typically formed in 4H and 6H SiC depending on the etching conditions (Fig. 1). Preliminary results for GaN growth on porous GaN have shown some promise for improved GaN quality [2-4]. It has been speculated that a porous surface may serve as a template for nano-scale lateral epitaxial overgrowth [4], and that a porous substrate layer may be compliant to any lattice and thermal mismatch strains [2-4]. In this work we grew GaN films on both porous SiC and GaN templates and evaluated the effect of using the porous template. Transmission electron microscopy (TEM), electron diffraction, x-ray diffraction (XRD), stylus profilometry, and photoluminescence were used to characterize the structural quality and defect density of the overgrown layers.

We employ plasma-assisted molecular beam epitaxy (PAMBE) to grow the GaN films on porous SiC, and both PAMBE and metalorganic chemical vapor deposition (MOCVD) for the growth on porous GaN. For the GaN/SiC heteroepitaxy the results are compared with that obtained for GaN growth on nonporous (regular) SiC, in which our

prior work has demonstrated state-of-the-art results in terms of structural quality [8]. The porous SiC substrates contain a thin skin layer about 50 nm in thickness with few exposed pores at the surface. As shown in a bright-field, cross-sectional TEM image in Fig. 1, the pores start to form a dense network only below this skin layer. For growth on the porous network, this skin layer must be removed prior to the growth. High temperature H-etching was used for this purpose in the present study, although this process was found to significantly enlarge the pores and modify the pore morphology [9]. Reactive ion beam etching may be a better procedure for skin removal [9].

II. EXPERIMENTAL

The porous 4H and 6H SiC substrates used in our experiments were purchased from TDI, Inc. The substrate treatment, growth temperatures, and thicknesses of the GaN layers grown are listed in Table 1. Samples C-1 and C-2 are two halves of the same substrate, with the C-2 half being porous. Hydrogen etching was performed at 1700°C and 1 atm pressure for various durations; for sample A, a 10 min H-etch was performed to completely remove polishing damage [10] whereas in samples B and C, a brief H-etching was performed in an effort to remove the skin layer above the porous network (although this removal was found to be incomplete, as seen in the TEM images below).

The porous GaN layers were produced using an electroless etching technique described in Ref. [6]. Following etching, the wafers are ultrasonically cleaned in water to remove any debris from the etching process. For the PAMBE overgrowth described below, the etching was done on PAMBE-grown GaN on SiC. For the MOCVD overgrowth, the etching was performed on GaN films purchased from TDI, Inc. consisting of GaN grown by hydride vapor phase epitaxy (HVPE) on sapphire. For PAMBE growth, temperatures of 750-800°C and Ga/N flux ratios of 1.1–1.5 were used. Details of the growth method can be found in Ref. [8]. MOCVD growth was performed using trimethyl gallium and ammonia in a vertical flow rotating substrate system, at temperatures near 1050°C [11]. All layers were examined in a JEOL JEM-200CX transmission electron microscope operating at 200 kV.

III. RESULTS AND DISCUSSION

A. GaN on porous SiC

In prior work we have studied in detail GaN growth by PAMBE on nonporous substrates [8,12,13]. To achieve a minimum dislocation density, films are grown with a Ga/N ratio which is only slightly greater than unity. Such films have a facetted morphology, and the dislocations tend to cluster in valleys of the surface morphology thereby reducing their relative separation and increasing the probability of annihilation. Sample A in Table 1 was grown on a nonporous substrate under such slightly Ga-rich conditions (Ga/N flux ratio of about 1.1). The defect density in this film is close to minimal as indicated by the XRD rocking curves [8]. From the plan-view image of this sample [13] we derive that the dislocation density in the top GaN layer is $1.1 \times 10^9/\text{cm}^2$ (with a <6% error).

During the initial stage of MBE growth of GaN on porous substrates, no growth is observed directly on top of exposed pores, as illustrated in Fig. 2(a) for sample B. The open tube thus formed in GaN can extend to a few hundred nanometers before it is closed. The extension of a GaN tube reflects a low lateral epitaxial growth rate of MBE

as compared to the vertical growth rate. Since the growth was carried out under a Ga-rich condition, most of the surface pores and some tubes were filled with Ga. Threading dislocations were observed to emerge from the surface pores as well as from areas in-between pores [Fig. 2(b)]. As in the case of non-porous growth (sample A), dislocation annihilation and combination occurred during growth, resulting in fewer dislocations in the upper part of the film.

Sample C-2, which was grown simultaneously on the porous half of the same 6H SiC substrate as sample C-1, shows growth behavior similar to that of sample B. The growth was performed at a lower growth temperature than samples A and B, and we found numerous Ga droplets on the GaN surface and more pronounced filling of Ga in surface pores and tubes [Fig. 3]. Nevertheless, Fig. 3 reveals dislocation behavior identical to that of samples A and B: clustering of dislocations toward recessed surface dimple areas and constant annihilations/combinations of them along the growth. Direct counting of dislocations in plan-view images indicates that the dislocation density in the top layer is lower in sample C-2 than in sample C-1 by about a factor of two ($1.9 \times 10^9/cm^2$ vs. $5.0 \times 10^9/cm^2$). Comparing sample B (on porous 4H SiC) with sample A (on non-porous 6H SiC), grown under the same conditions, showed similar dislocation reduction.

Besides low defect density, full relaxation of lattice-mismatch and thermal-mismatch induced strains is also important, particularly for large-area growth. Selected area electron diffraction can be used to measure the relative film/substrate lattice constants if the effect of small c-axis tilt and rotation can be ignored. However, one has to be careful in deriving the $\Delta a/a$ or $\Delta c/c$ values directly from a diffraction pattern, since a slight GaN lattice tilt or rotation relative to the substrate in an Ewald sphere construction will cause a shift in the positions of diffraction spots. Plan-view diffraction patterns obtained in this study indicate that the GaN c-axis rotation is very small (< 0.25°), and the measured $\Delta a/a$ values listed in Table 1 should be reliable to about 0.1%. In Fig. 4, we compare the diffraction patterns taken from the nonporous (C-1) and porous growth (C-2). We find more relaxation, i.e. a larger $\Delta a/a$ value, in a film grown on a porous substrate (Table 1). Similarly, sample B is slightly more relaxed than sample A. The $\Delta a/a$ of sample C-2 (3.7%) exceeds the strain free value of 3.48% (assuming bulk values for the lattice constants [15]), suggesting that the film is in tension (perhaps because of the additional thermal-mismatch strain introduced during the cooling from the growth temperature to room temperature [16]). We have confirmed the trend of these strain results based on TEM with measurements of wafer curvature using stylus profilometry. We find sample A to have large compression with radius of curvature of 1.2 m implying a $\Delta a/a$ value of 0.10% less than the strain-free value, whereas samples B, C-1, and C-2 have relatively little strain (R>10 m) and/or are slightly in tension.

It is important to note that, although the growths on porous and nonporous substrates were performed under nominally identical conditions, we observe for a fixed heater current during growth that the substrate temperature on the porous wafers is somewhat higher, by about 30-40°C for the growth temperatures used here [14]. Some of the differences we find between the growth on porous and nonporous substrates may arise from this factor, since a change in temperature will change the effect Ga/N flux ratio, which in turn affects the structural quality of the GaN [8].

B. GaN on porous GaN

Figure 5 shows results of the PAMBE overgrowth of GaN films on porous GaN. The layer which was etched to produce the porous template, which we will refer to as the *seed layer*, was for these experiments a GaN film with thickness of 1-2 μm grown by PAMBE. These layers typically have threading dislocation densities of about 3×10^{9} cm^{-2} for edge dislocations and 1×10^{8} cm^{-2} for screw dislocations, with very few dislocations of mixed character [8,12]. The seed film for the sample shown in Fig. 5 was etched for 10 min producing a 0.25 μm thick porous layer as indicated by the arrows in Fig. 5. As seen in Fig. 6 (and in other, higher magnification images) these pores extend vertically, with typical diameter of about 20 nm. Dislocations existing in the seed layer are seen to propagate through the porous layer and into the overgrown film. We thus find quite similar structural quality of the seed layers and the overgrown films. This similarity is confirmed by XRD, which reveals the same values of rocking curve widths, within 20%, for the seed layers and the overgrown films. Thus the porous template is found to induce neither dislocation annihilation nor dislocation generation, to any significant degree.

Results for MOCVD overgrowth on porous GaN layers are shown in Figs. 7 and 8. The seed layer in this case is a layer grown by HVPE, with thickness of about 4 μm and having threading dislocation density, particularly for screw or mixed dislocations, considerably higher than that of the PAMBE seed layer discussed above. This seed film was etched for 15-45 min to produce the porous layers, resulting in pores with diameter of 50-80 nm. A MOCVD film with thickness of 4 μm was then grown on the porous template. As seen in both Figs. 7 and 8, the overgrown film has a dramatically reduced dislocation density, with 5-10× fewer dislocations than the seed layer. In Fig. 8 one can clearly see that the dislocations from the seed layer propagate through the porous layer and then, in the first few hundred nm of the overgrown layer they annihilate each other. This enhanced annihilation in the MOCVD layer implies that the dislocations are not propagating uniformly upwards during the film growth, but rather, they move laterally and thereby encounter other nearby dislocations and combine or annihilate.

The improved structural quality of the MOCVD films compared to the seed layers is also revealed by XRD. Table 2 shows results for two groups of samples. Samples E and F were overgrown and characterized by XRD after the overgrowth, with sample D being a control sample which was not overgrown. The reduction in the rocking curve widths for sample E and F compared to D, particularly for the (0002) reflection which is sensitive to dislocations with screw or mixed character, is evident. The second group of samples in Table 2, G, H, and I, were characterized by XRD both before and after overgrowth, with the control sample in this case, sample G, having the etching step skipped so that it does not have a porous layer. It is clear from these results that the overgrowth produces a significant reduction in the FWHM of the rocking curves, consistent with the reduced dislocation density seen by TEM. However, importantly, we find a similar reduction in dislocation density even for sample G, which did *not* have a porous layer. A TEM image of that sample is shown in Fig. 9, revealing significant dislocation annihilation in the first few hundred nm of the MOCVD-grown layer. Thus, the dislocation annihilation is not determined by the porous template, but rather, it appears to be determined by the properties of the evolving MOCVD-grown layer itself. As mentioned above, some lateral movement of the dislocations evidently takes place during growth (i.e. due to lateral growth of the film, or perhaps from some strain related

mechanism which induces glide of the dislocations) which results in dislocation combination and/or annihilation.

IV. CONCLUSION

We have investigated the growth of GaN on porous SiC and GaN substrates. For the growth on porous SiC, using PAMBE, we have observed reductions of roughly a factor of two in dislocation density as compared to conventional growth on non-porous SiC substrates under the same growth conditions. We have also noticed a tendency for growth on porous substrates to produce films that are slightly more relaxed than those of the corresponding non-porous growth. In both porous and non-porous growths, the dislocation density decreases with the GaN layer thickness through a dislocation combination/annihilation mechanism. At the initial stage of growth on porous material, because of limited lateral growth, open tubes a few hundred nanometers long are formed on top of the SiC surface pores. These surface pores and tubes trap Ga droplets under a Ga-rich growth condition or at lower growth temperatures. The mechanisms responsible for the slight reduction in dislocation density and for the increased strain relaxation observed in porous growth are not clear. These two effects might be related. It is possible that the surface pores and the extended tubes can act as convenient dislocation sources to provide misfit dislocation to relax the misfit strain. The open tubes with free surfaces may also serve as sinks to trap threading dislocations.

Growth on porous GaN has been performed by both PAMBE and MOCVD. In the former case the overgrown films are found to replicate the dislocation structures existing in the seed film below the porous layer. Similar dislocation densities exist in the overgrown layers as compared with the seed layer. Using MOCVD, a reduction in dislocation density of 5-10× in the overgrown film as compared with the seed layer is found. However, this reduction occurs even in the absence of the porous template layer, thus demonstrating that the porous template is not responsible for the improvement in the structural quality. Rather, the dislocation annihilation appears to be a result of dislocation glide during the evolution of the MOCVD layer.

ACKNOWLEDGMENTS

This work was supported by a Defense University Research Initiative on Nanotechnology (DURINT) program administered by the Office of Naval Research under Grant N00014-01-1-0715 (program monitor Dr. Colin Wood). The work at Sandia is partially supported by the Division of Materials Science and Engineering, Office of Basic Energy Sciences, US DOE. Sandia is a multiprogram laboratory operated by Sandia Corporation, a Lockheed Martin Company, for the U.S. Department of Energy under Contract No. DE-AC04-94AL85000.

REFERENCES

1. S. E. Saddow, M. Mynbaeva, W. J. Choyke, S. Bai, G. Melnychuk, Y. Koshka, V. Dimitriev and C. E. C. Wood, Materials Science Forum **353 –356**, 115 (2001) .
2. M. Mynbaeva, A. Titkov, A. Kryzhanovski, V. Ratnikov, H. Huhtinen, R. Laiho and V. Dmitriev, Appl. Phys. Lett. **76**, 1113 (2000).
3. M. Mynbaeva, A. Titkov, A. Kryzhanovski, I. Kotousova, A. S. Zubrilov, V. V. Ratnikov, V. Yu. Davydov, N. I. Kuznetsov, K. Mynbaev, D. V. Tsvetkov, S. Stepanov, A. Cherenkov, and V. Dmitriev, MRS Internet J. Nitride Semicond. Res. **4**, 14 (1999).
4. M. Mynbaeva, A. Titkov, A. Kryzhanovski, A. Zubrilov, V. Ratnikov, V. Davydov, N. Kuznetsov, K. Mynbaev, S. Stepanov, A. Cherenkov, I. Kotousova, D. Tsvetkov, V. Dmitriev, Mat. Res. Soc. Symp. Vol. 595, W2.7.1 (2000).
5. G. Melnychuk, M. Mynbaeva, S. Rendakova, V. Dmitriev and S. E. Saddow, Mat. Res. Soc. Symp. Vol. 622, T4.2.1 (2000).
6. X. Li, Y.-W. Kim, P. W. Bohn, and I. Adesida, Appl. Phys. Lett. **80**, 980 (2002).
7. J. S. Shor, I. Grimberg, B. -Z. Weiss and A. D. Kurtz, Appl. Phys. Lett. **62**, 2836 (1993).
8. C. D. Lee, A. Sagar, R. M. Feenstra, C. K. Inoki, T. S. Kuan, W. L. Sarney, and L. Salamanca-Riba, Appl. Phys. Lett. **79**, 3428 (2001).
9. A. Sagar, C. D. Lee, R. M. Feenstra, C. K. Inoki, and T. S. Kuan, J. Appl. Phys., **92** 4070 (2002).
10. V. Ramachandran, M. F. Brady, A. R. Smith and R. M. Feenstra, J. Electron. Mat. **27**, 308 (1998).
11. D. D. Koleske, A. J. Fischer, A. A. Allerman, C. C. Mitchell, K. C. Cross, S. R. Kurtz, J. J. Figiel, K. W. Fullmer, and W. G. Breiland, Appl. Phys. Lett. **81**, 1940 (2002).
12. C. D. Lee, V. Ramachandran, Ashutosh Sagar, R. M. Feenstra, D. W. Greve, W. L. Sarney, L. Salamanca-Riba, D. C. Look, Song Bai, W. J. Choyke, and R. P. Devaty, J. Electron. Mat. **30**, 162 (2001).
13. C. K. Inoki, T. S. Kuan, C. D. Lee, Ashutosh Sagar, and R. M. Feenstra, Mat. Res. Soc. Symp. Proc. Vol. **722**, K1.3.1 (2002).
14. This increased temperature of the porous layer is clearly evidenced by the resulting morphology of the GaN overgrown layers (see Ref. [9] for additional discussion). An increased temperature of porous SiC would be consistent with an expected reduced thermal conductivity of the material, i.e. similar to that known for porous Si which has a thermal conductivity 1-2 orders of magnitude lower than that of nonporous Si (see, e.g., S. Perichon et al., Diffus. Defect Data B, Solid State Phenom. **80-81**, 417 (2001)).
15. It is possible that the SiC lattice constant changes when the material is made porous. For example, porous Si is found to have a *larger* lattice constant than nonporous Si (K. Barla, R. Herino, G. Bomchil, and J. C. Pfister, J. Cryst. Growth **68**, 727 (1984)).
16. P. Waltereit, O. Brandt, A. Trampert, M. Ramsteiner, M. Reiche, M. Qi, and K. H. Ploog, Appl. Phys. Lett. **74**, 3660 (1999).

Table 1 Growth conditions, strain relaxation, and defect density for MBE-grown GaN on SiC.

Sample	SiC substrate	T_{growth}, Ga/N flux ratio, GaN thickness	Strain relaxation	Dislocation density in top layer
A	6H, (0001) H-etched, 1700°C/10 min	800°C, 1.1 1.9 μm	~97% (Δa/a~3.4%) GaN in compression	1.1×10^9/cm^2
B	Porous 4H, 8° off (0001) H-etched, 1700°C/1 min	800°C, 1.1 1.6 μm	~100% (Δa/a~3.5%)	5.8×10^8/cm^2
C-1	6H, 3.5° off (0001) H-etched, 1700°C/2 min	750°C, 1.5 0.95 μm	~100% (Δa/a~3.5%)	5.0×10^9/cm^2
C-2	Porous 6H, 3.5° off (0001) H-etched, 1700°C/2 min	750°C, 1.5 0.95 μm	~100% (Δa/a~3.7%) GaN in tension	1.9×10^9/cm^2

Table 2 Etching time and x-ray diffraction rocking curve widths (FWHM, arcsec) for MOCVD-grown GaN on GaN.

Sample	etching time	HVPE GaN seed		MOCVD GaN overgrowth	
		(0002)	$(10\bar{1}2)$	(0002)	$(10\bar{1}2)$
D	no etch	434	581	--	--
E	15 min	--	--	250	485
F	45 min	--	--	289	494
G	no etch	408	776	260	617
H	15 min	374	690	247	558
I	45 min	468	747	291	585

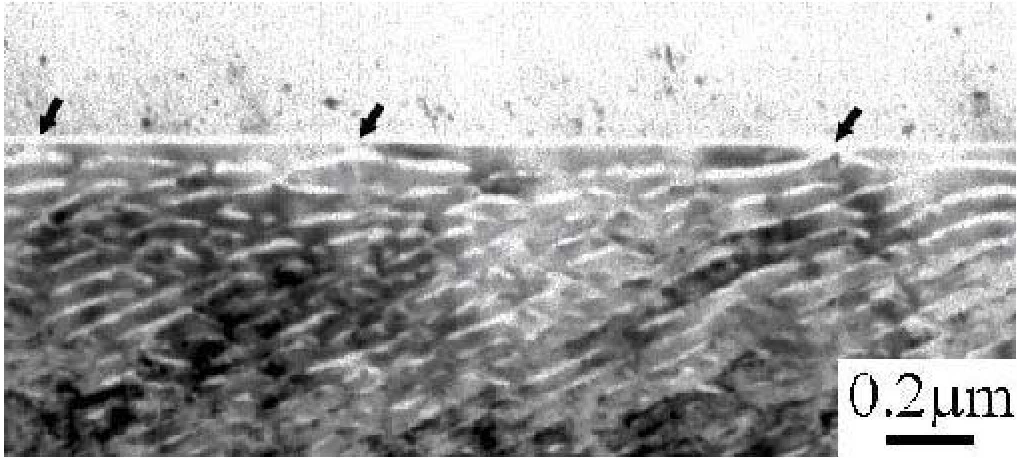

Fig. 1. Cross-sectional TEM image of a porous 6H-SiC substrate indicating the presence of a top skin layer. The density of exposed surface pores, as marked by arrows, is very low.

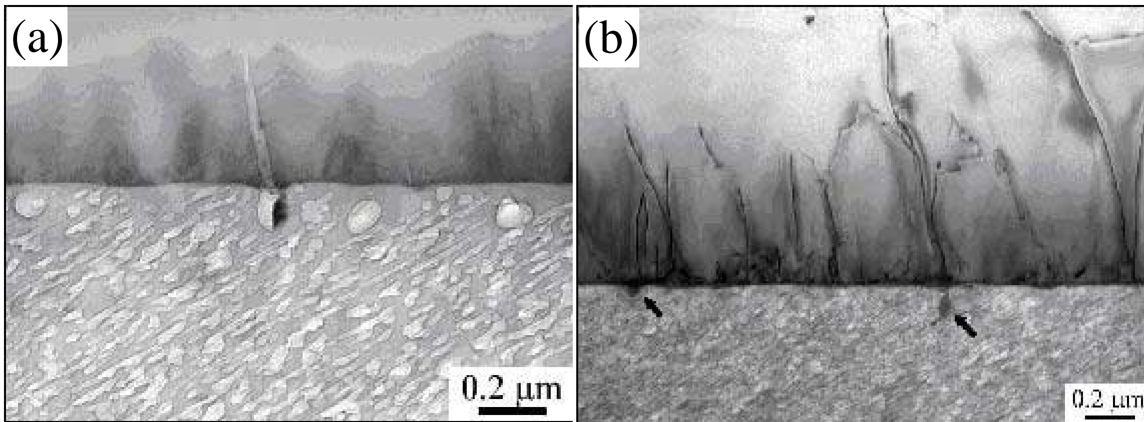

Fig. 2 (a) A cross-sectional TEM image of GaN film on porous SiC (sample B) showing an exposed pore filled with Ga, and an open tube extended from the pore. (b) Another image of the same sample showing dislocations emerging from Ga-filled surface pores (arrows), as well as from areas in-between surface pores.

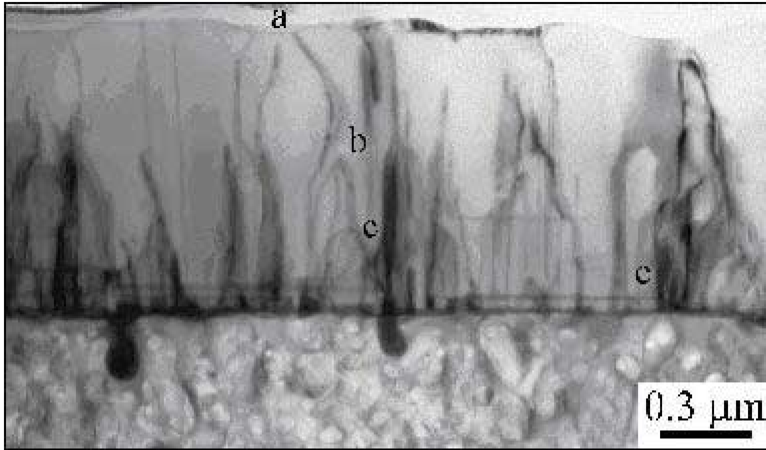

Fig. 3 A cross-sectional, bright-field image of GaN film on porous SiC (sample C-2) showing threading dislocations bending toward a surface valley [a] and some of them annihilating each other [b]. Open tubes partially filled with Ga are also observed on top of surface pores [c].

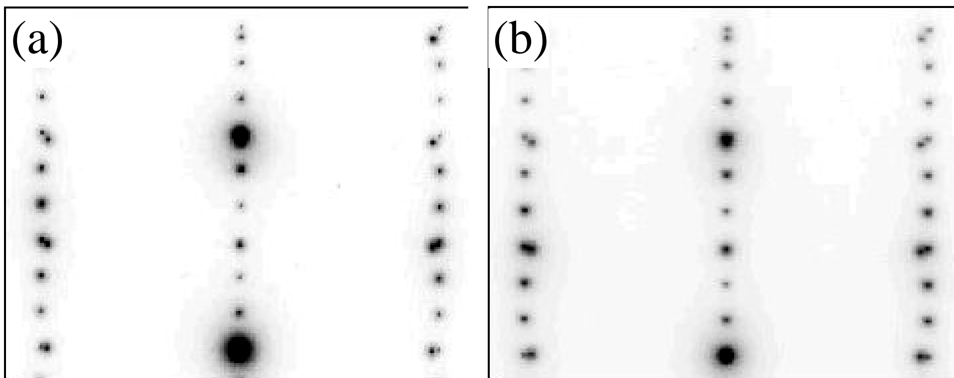

Fig. 4 Diffraction patterns taken from GaN on: (a) sample C-1 grown on nonporous SiC and (b) sample C-2 grown on porous GaN.

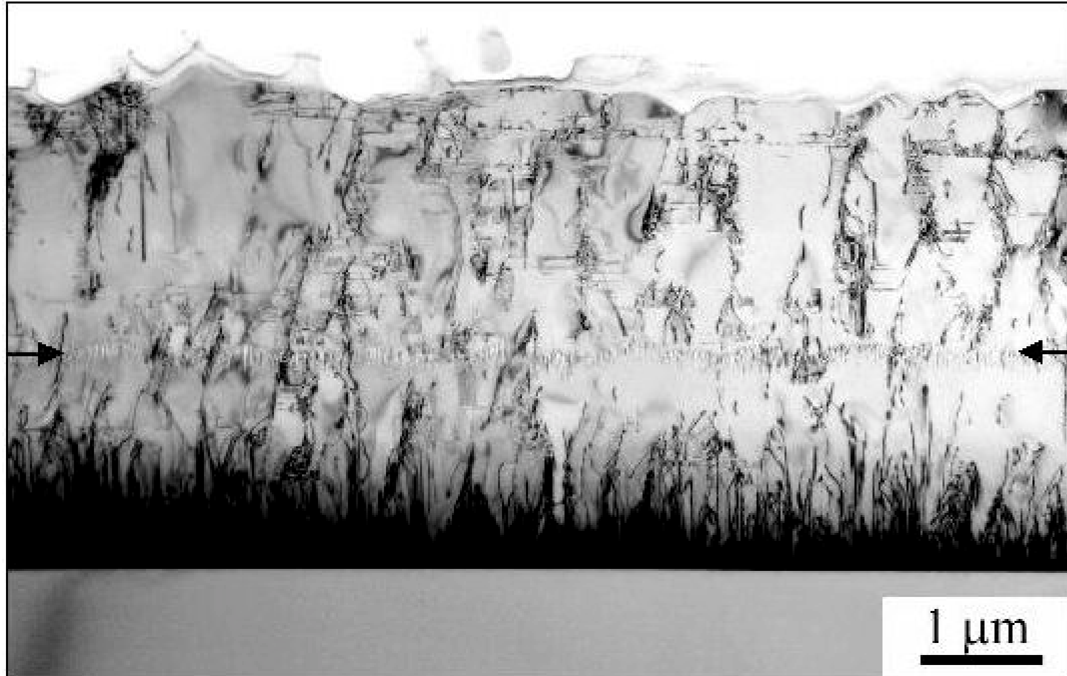

Fig. 5 GaN film grown by PAMBE on porous GaN. The black arrows indicate the location of the porous layer.

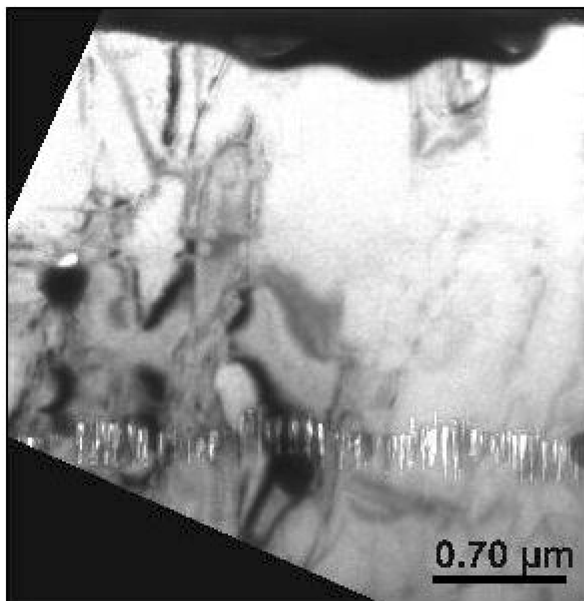

Fig. 6 GaN film grown by PAMBE on porous GaN (same sample as in Fig. 5). This TEM specimen was thinned by a focussed ion beam (FIB), yielding relatively uniform thickness of the specimen.

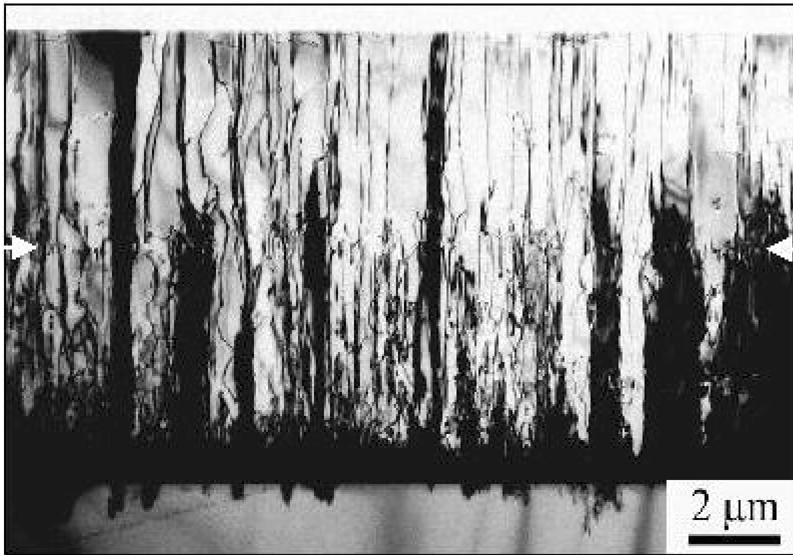

Fig. 7 Cross-sectional TEM image of a GaN film grown by MOCVD on porous GaN (sample E). The white arrows indicate the location of the porous layer.

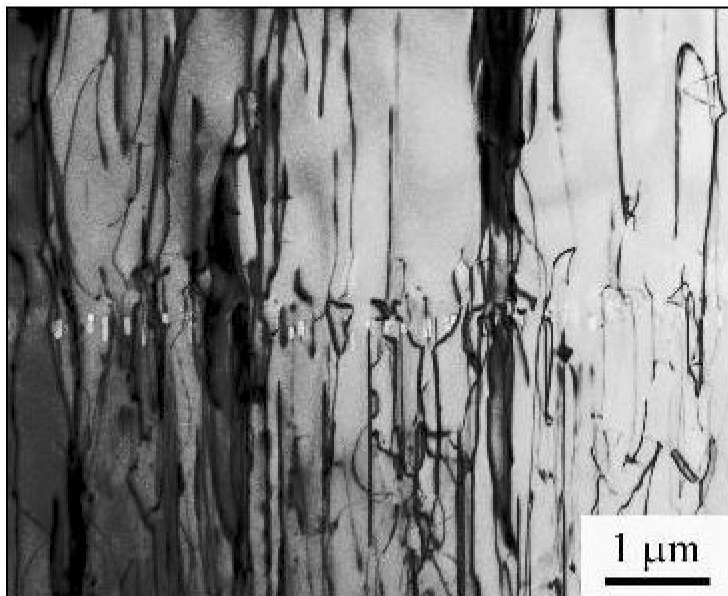

Fig. 8 Expanded view of GaN film grown by MOCVD on porous GaN (sample E).

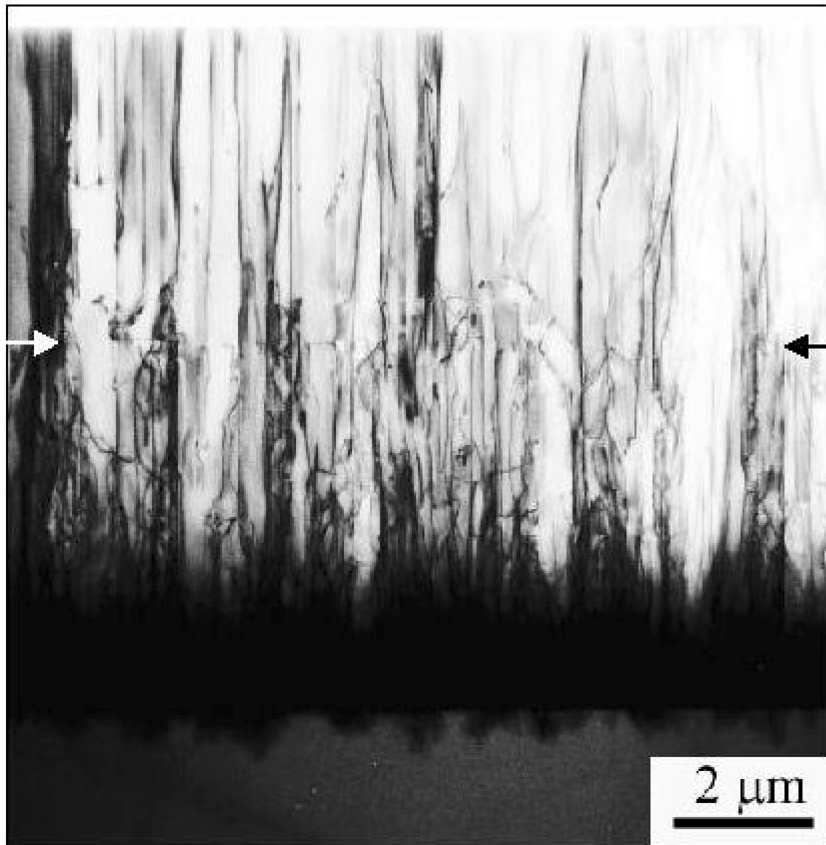

Fig. 9 Cross-sectional TEM image of a GaN film grown by MOCVD on seed layer (sample G), but without the presence of a porous layer. The black and white arrows indicate the location of the interface between MOCVD- and HVPE-grown material.